

Variations on a WIMP

Patrick Stengel

University of Hawaii

October 1, 2015

(1404.6599), 1511.03728 with Nicolas Fernandez,
(Jason Kumar) and Ilsoo Seong
1411.2643 with Chris Kelso, Jason Kumar and Pearl Sandick
1510.XXXXX with Keith Dienes, Jason Kumar and Brooks Thomas

- 1 Introduction
- 2 Searches for Light Dark Matter at High Luminosity Colliders
 - Model Independent Constraints on Effective Operators
 - Single Photon Decays of Heavy Quarkonium
 - Results and Analysis
- 3 A Strange Brew in the Incredible Bulk
 - Model Framework
 - Strange Squark Scattering
 - Sensitivity of Direct Detection
- 4 Cosmological Constraints on Decaying Ensembles
 - Single Component DM and Multicomponent DM
 - Light Element Abundances
- 5 Summary and Outlook

WIMP miracle predicts new physics at the weak scale

Stable, thermally produced particle will freeze out with relic abundance

$$\Omega_X \sim 1/\langle\sigma_{AV}\rangle$$

largely independent of DM mass, m_X

Assuming a weak coupling, dimensionally, the cross section

$$\langle\sigma_{AV}\rangle \sim \frac{g_{weak}^4}{m_X^2} (1 \text{ or } v^2)$$

$m_X \sim m_{weak}$ will yield the correct Ω_{DM} for s - or p -wave annihilation

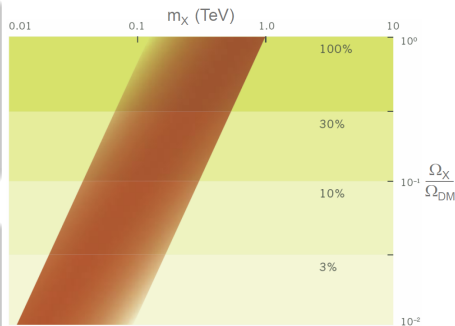


Figure: Fraction of dark matter density for thermal relic dark matter of mass m_X . Width from s - or p -wave annihilations and deviations from assumptions, see Feng 1003.0904.

Weak scale DM motivated by new physics models

Stabilize gauge hierarchy problem \rightarrow
new weak scale particles

- Lightest new particle protected by discrete symmetry
- Provides WIMP candidate

Neutralino in MSSM

- Mixture of neutral gauginos and higgsinos
- SM interactions depend on specific model
- mSUGRA tightly constrained

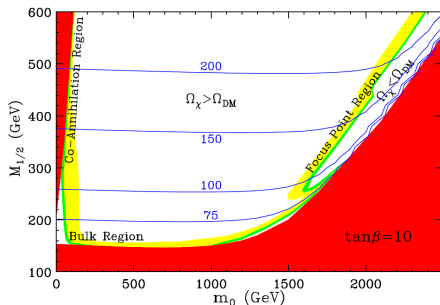


Figure: Cosmologically preferred mSUGRA regions are in green with $A_0 = 0$ and $\mu > 0$. Blue contours denote neutralino masses, see Feng 1003.0904.

Possible DM signatures and alternative phenomenology

SM SM \rightarrow DM DM

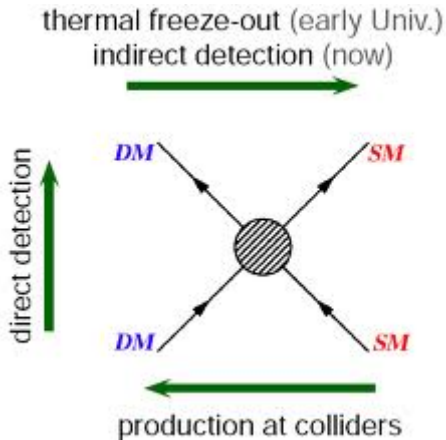
- Missing energy at LHC
- $m_{\chi} \lesssim 10 \text{ GeV}$ at e^+/e^-

DM SM \rightarrow DM SM

- Observe nuclear recoils
- Limited by E_{thr} , uncertainties
- L-R strange squark mixing

DM DM \rightarrow SM SM

- DM annihilates today
- Dynamical dark matter ensemble can inject significant energy during early universe



Outline

- 1 Introduction
- 2 Searches for Light Dark Matter at High Luminosity Colliders
 - Model Independent Constraints on Effective Operators
 - Single Photon Decays of Heavy Quarkonium
 - Results and Analysis
- 3 A Strange Brew in the Incredible Bulk
 - Model Framework
 - Strange Squark Scattering
 - Sensitivity of Direct Detection
- 4 Cosmological Constraints on Decaying Ensembles
 - Single Component DM and Multicomponent DM
 - Light Element Abundances
- 5 Summary and Outlook

Model independent constraints from contact interactions

Name	Interaction Structure	σ_{SI} suppression	σ_{SD} suppression	s-wave?
F1	$\bar{X} X \bar{q} q$	1	$q^2 v^{1.2}$ (SM)	No
F2	$\bar{X} \gamma^5 X \bar{q} q$	q^2 (DM)	$q^2 v^{1.2}$ (SM); q^2 (DM)	Yes
F3	$\bar{X} X \bar{q} \gamma^5 q$	0	q^2 (SM)	No
F4	$\bar{X} \gamma^5 X \bar{q} \gamma^5 q$	0	q^2 (SM); q^2 (DM)	Yes
F5	$\bar{X} \gamma^\mu X \bar{q} \gamma_\mu q$ (vanishes for Majorana X)	1	$q^2 v^{1.2}$ (SM) q^2 (SM); q^2 or $v^{1.2}$ (DM)	Yes
F6	$\bar{X} \gamma^\mu \gamma^5 X \bar{q} \gamma_\mu q$	$v^{1.2}$ (SM or DM)	q^2 (SM)	No
F7	$\bar{X} \gamma^\mu X \bar{q} \gamma_\mu \gamma^5 q$ (vanishes for Majorana X)	$q^2 v^{1.2}$ (SM); q^2 (DM)	$v^{1.2}$ (SM) $v^{1.2}$ or q^2 (DM)	Yes
F8	$\bar{X} \gamma^\mu \gamma^5 X \bar{q} \gamma_\mu \gamma^5 q$	$q^2 v^{1.2}$ (SM)	1	$\propto m_\gamma^2 / m_X^2$
F9	$\bar{X} \sigma^{\mu\nu} X \bar{q} \sigma_{\mu\nu} q$ (vanishes for Majorana X)	q^2 (SM); q^2 or $v^{1.2}$ (DM) $q^2 v^{1.2}$ (SM)	1	Yes
F10	$\bar{X} \sigma^{\mu\nu} \gamma^5 X \bar{q} \sigma_{\mu\nu} q$ (vanishes for Majorana X)	q^2 (SM)	$v^{1.2}$ (SM) q^2 or $v^{1.2}$ (DM)	Yes

Figure: All possible Lorentz invariant dimension 6 operators for fermionic DM interacting with quarks [arXiv:1305.1611]. Interaction strength will be set by Wilson coefficient, $1/\Lambda^2$ or m_q/Λ^3 , with Λ the mass scale of UV physics. Also lists any velocity or momentum suppression of scattering or annihilation cross sections.

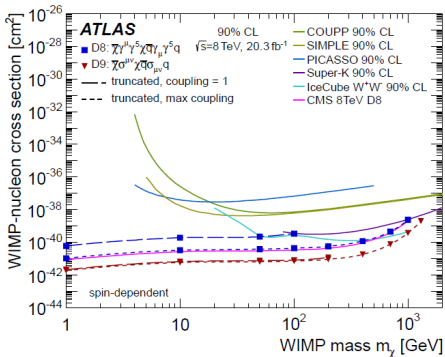
$$pp \rightarrow X\bar{X}j, pp \rightarrow X\bar{X}\gamma, pp \rightarrow X\bar{X}W/Z \text{ at LHC}$$


Figure: Inferred limits on SD scattering cross section from ATLAS monojet search. Competitive with direct detection without A^2 enhancement and probes lower mass region.

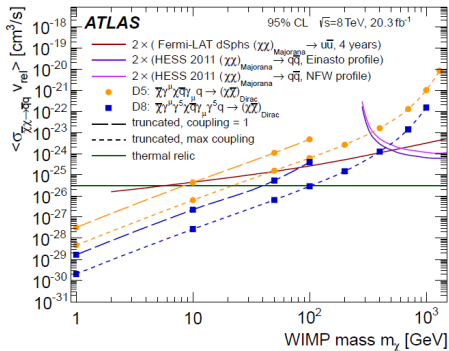
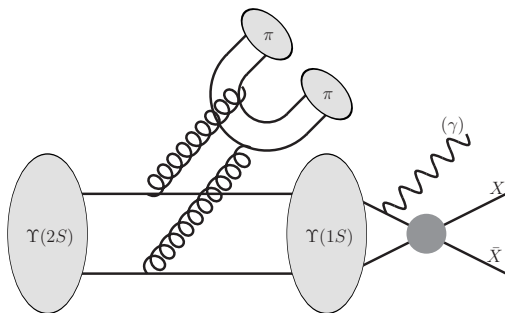


Figure: Inferred limits on DM annihilation rate from same search. Can rule out thermal relic annihilating only to light quarks through F5 or F8 at low m_χ , ATLAS 1502.01518

Quarkonium decays to light dark matter (LDM)



LDM at e^+/e^- colliders

- Directly probe couplings of DM to heavy flavor quarks
- Arises in NMSSM with light A see Gunion et. al. hep-ph/0509024

Complements LHC searches

- Unitary down to $\Lambda \sim 10$ GeV rather than $\mathcal{O}(\text{TeV})$ at LHC
- Differentiate operators based on initial/final state

Standard Model bilinears for $\Upsilon(1S)$ (and J/ψ) decays

bilinear	C	P	J	state
$\bar{\psi}\psi$	+	+	0	$S = 1, L = 1$
$i\bar{\psi}\gamma^5\psi$	+	-	0	$S = 0, L = 0$
$\bar{\psi}\gamma^0\psi$	-	+	0	none
$\bar{\psi}\gamma^i\psi$	-	-	1	$S = 1, L = 0, 2$
$\bar{\psi}\gamma^0\gamma^5\psi$	+	-	0	$S = 0, L = 0$
$\bar{\psi}\gamma^i\gamma^5\psi$	+	+	1	$S = 1, L = 1$
$\bar{\psi}\sigma^{0i}\psi$	-	-	1	$S = 1, L = 0, 2$
$\bar{\psi}\sigma^{ij}\psi$	-	+	1	$S = 0, L = 1$
$\phi^\dagger\phi$	+	+	0	$S = 0, L = 0$
$i\text{Im}(\phi^\dagger\partial^0\phi)$	-	+	0	none
$i\text{Im}(\phi^\dagger\partial^i\phi)$	-	-	1	$S = 0, L = 1$
$B_\mu^\dagger B^\mu$	+	+	0	$S = 0, L = 0; S = 2, L = 2$
$i\text{Im}(B_\nu^\dagger\partial^0 B^\nu)$	-	+	0	none
$i\text{Im}(B_\nu^\dagger\partial^i B^\nu)$	-	-	1	$S = 0, L = 1; S = 2, L = 1, 3$
$i(B_i^\dagger B_j - B_j^\dagger B_i)$	-	+	1	$S = 1, L = 0, 2$
$i(B_i^\dagger B_0 - B_0^\dagger B_i)$	-	-	1	$S = 0, L = 1; S = 2, L = 1, 3$
$\epsilon^{0ijk} B_i \partial_j B_k$	+	-	0	$S = 1, L = 1$
$-\epsilon^{0ijk} B_0 \partial_j B_k$	+	+	1	$S = 2, L = 2$
$B^\nu \partial_\nu B_0$	+	+	0	$S = 0, L = 0; S = 2, L = 2$
$B^\nu \partial_\nu B_i$	+	-	1	$S = 1, L = 1$

Purely invisible decays

- Use dipion system from hadronic transition to reconstruct $\Upsilon(1S)$, which then decays $\rightarrow \tilde{X}X$
- Need $J^{PC} = 1^{--} q\bar{q}$ bound states: Either $\bar{q}\gamma^i q$ or $\bar{q}\sigma^{0i} q$ couples to DM bilinear

Decays to invisible + γ

- Use single photon trigger to get missing mass distribution of $\tilde{X}X$
- Charge conjugation tells us we need $C = +$ bilinears, defines orthogonal set of operators

Complementary constraints on effective operators

Structure	Invisible	Radiative	s-wave	Scattering
F1 $(m_q/\Lambda^3)\bar{X}X\bar{q}q$	$(0^{++}, 1, 1)$	$(1^{--}, 1, 0)$ $(1^{+-}, 0, 1)$	No	SI
F4 $(m_q/\Lambda^3)\bar{X}\gamma^5 X\bar{q}\gamma^5 q$	$(0^{-+}, 0, 0)$	$(1^{--}, 1, 0)$ $(1^{+-}, 0, 1)$	Yes	No
F8 $(1/\Lambda^2)\bar{X}\gamma^\mu\gamma^5 X\bar{q}\gamma_\mu\gamma^5 q$	$(0^{-+}, 0, 0)$ $(1^{++}, 1, 1)$	$(1^{--}, 1, 0)$	Yes	SD

 $\Upsilon(1S) \rightarrow \gamma\bar{X}X$ related decays

Particular combinations of bound states and final states constrain operators with SM bilinears which can annihilate (J^{PC}, S, L) mesons
 $h_b(1P) \rightarrow \gamma\bar{X}X$, $\chi_{b0}(1P) \rightarrow \bar{X}X$,
 $\eta_b(1S) \rightarrow \bar{X}X$, $\chi_{b1}(1P) \rightarrow \bar{X}X$

Direct and indirect detection

- s-wave annihilation can yield constraints from dSphs and CMB ionization history
- Velocity independent spin-independent or dependent scattering off of nucleons

Approximate limits on decays though all possible operators

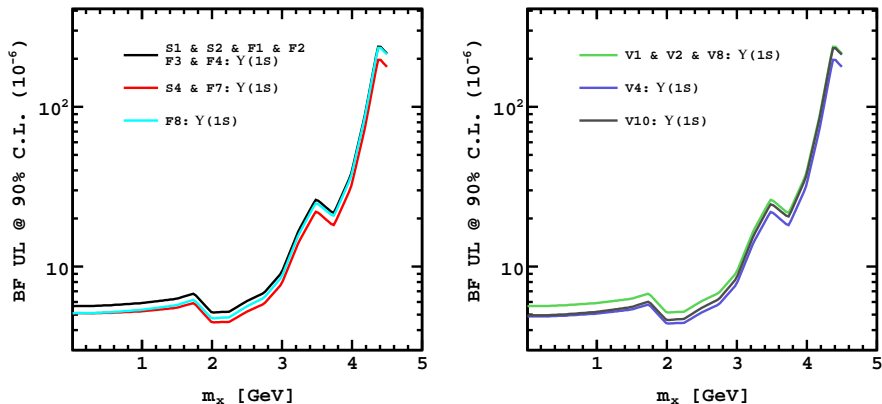


Figure: Limits on $\mathcal{B}(\gamma\bar{X}X)$ for contact operators that can mediate $\Upsilon(1S) \rightarrow \gamma\bar{X}X$ decays with scalar/fermionic (left) and vector (right) DM. Rescaling is more sensitive to geometric acceptance than photon energy threshold.

Limits on effective couplings along with dSphs and mono-X

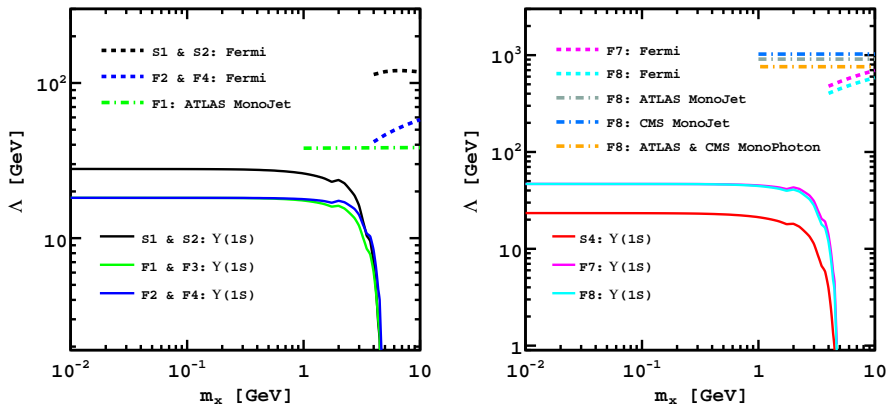
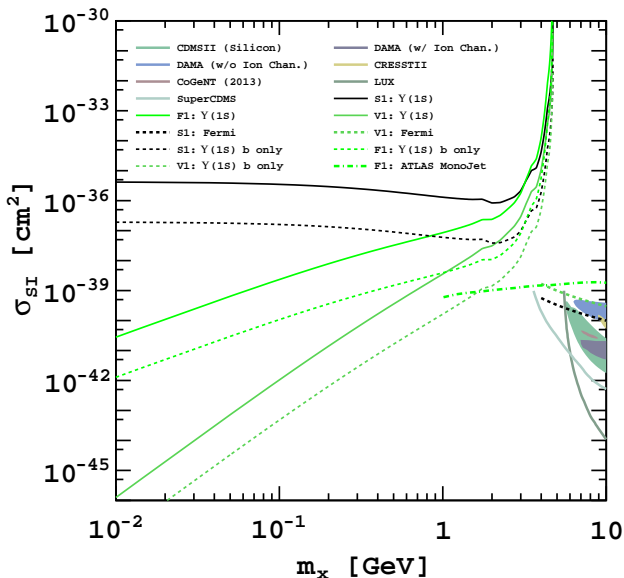


Figure: Limits on mediator scale, Λ , for contact operators with scalar/fermionic DM. Scalar/pseudoscalar mediated interactions (left) have effective couplings $m_q/\Lambda^{2,3}$ and interactions with pseudovector quark bilinears (right) have effective couplings $1/\Lambda^2$. **MFV-like couplings enhance constraints** from meson decays.

$\Upsilon(1S)$ complementary bounds on DM-p SI scattering

Outline

- 1 Introduction
- 2 Searches for Light Dark Matter at High Luminosity Colliders
 - Model Independent Constraints on Effective Operators
 - Single Photon Decays of Heavy Quarkonium
 - Results and Analysis
- 3 A Strange Brew in the Incredible Bulk
 - Model Framework
 - Strange Squark Scattering
 - Sensitivity of Direct Detection
- 4 Cosmological Constraints on Decaying Ensembles
 - Single Component DM and Multicomponent DM
 - Light Element Abundances
- 5 Summary and Outlook

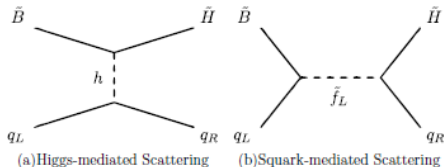
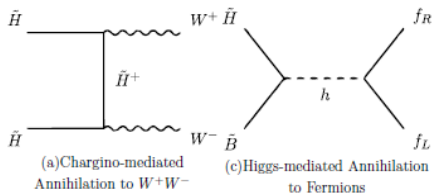
Typical mSUGRA/CMSSM scenario with $\tilde{B}-\tilde{H}$ admixture

Relic density with $\tilde{X}\tilde{X} \rightarrow WW, ff$

- Assuming gaugino mass unification (at least $M_1 \lesssim M_2$), yields neutralino with small \tilde{W}
- Minimal flavor violation eliminates sfermion mixing
- Need $\mu/m_X \sim \mathcal{O}(1)$ for s -wave see e.g. Feng, Sanford 1009.3934

SI scattering with Higgs exchange

- Scalar mediated interactions are velocity independent
- Minimal flavor violation guarantees coupling $\sim m_q$
- LHC data and $m_h \simeq 125$ GeV push unified $m_{\tilde{f}} \gtrsim \mathcal{O}(\text{TeV})$ see e.g. Baer et. al. 1112.3017



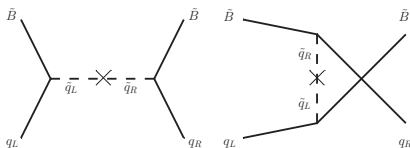
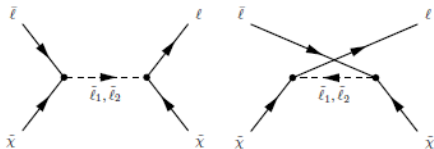
Resurrect "bulk" region by relaxing MFV, allowing light \tilde{f}

DM depletes with slepton exchange

- Pure \tilde{B} need sfermions with L-R mixing, nondegenerate masses for s -wave annihilation
- Limits only $m_{\tilde{\tau}} \gtrsim \mathcal{O}(100 \text{ GeV})$
- Need to check constraints on dipole moment contributions see Fukushima et. al. 1406.4903

SI scattering with squark exchange

- Decoupled gluinos with one non-degenerate light flavor squark $m_{\tilde{q}_1} \gtrsim \mathcal{O}(500 \text{ GeV})$
- Lower $m_{\tilde{g}}$ increases t -channel \tilde{g} contribution, constrains 1st generation more than 2nd
- Gauge coupling $\sim \sin 2\phi_{\tilde{q}}$



Squark limits for universal and non-degenerate masses

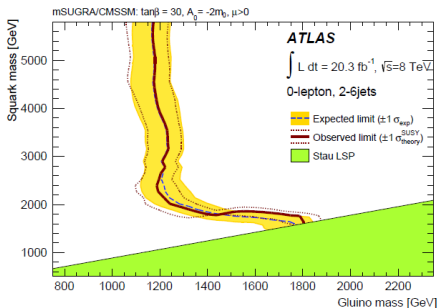


Figure: Interpretation of squark/gluino search in final states with jets plus MET within the CMSSM. Results shown in the $(m_{\tilde{g}}, m_{\tilde{q}})$ -plane from a scan over $0 < m_0 < 6 \text{ TeV}$ and $300 \text{ GeV} < m_{1/2} < 900 \text{ GeV}$.

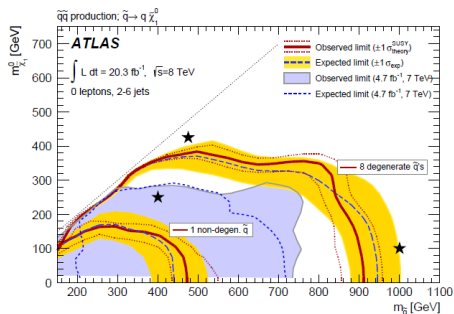


Figure: Interpretation of same search within simplified models only considering production of light flavor squark pairs. Gluinos are assumed to be decoupled, so s-channel gluon dominates production, see ATLAS 1405.7875

PDF suppression of 2nd generation squark production

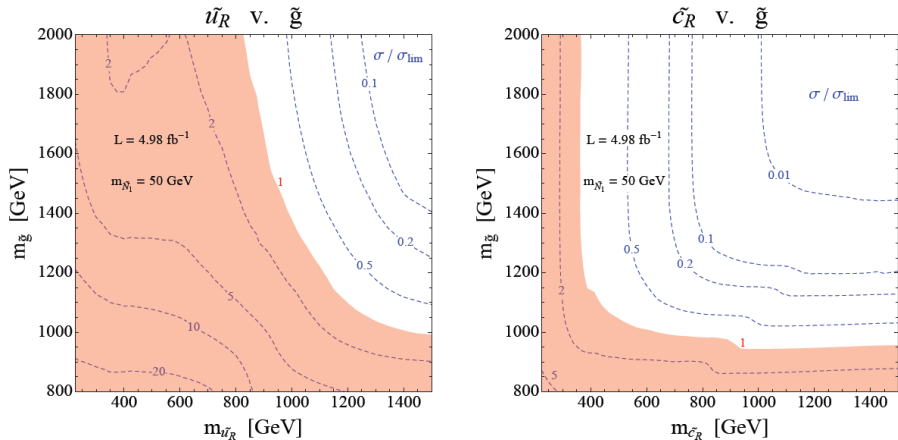


Figure: As $m_{\tilde{g}}$ falls, t -channel gluino exchange becomes important and the cross section for production 1st generation squarks is enhanced relative to 2nd, yielding weaker constraints on 2nd generation squark masses, Mahbubani et. al.

1212.3328.

Scattering through scalar exchange in non-relativistic limit

$$\sigma_{SI}^N = \frac{\mu_p^2}{32\pi(2J_X + 1)} \sum_{spins} \left| \sum_q \frac{B_q^N}{m_X m_q} \mathcal{M}_{Xq \rightarrow Xq} \right|^2$$

$$B_q^N = \langle N | \bar{q}q | N \rangle = m_N f_q^N / m_q$$

$$B_u^P = B_d^n = \tilde{\Sigma}_{\pi N} \left[1 + (1 - y) \left(\frac{z - 1}{z + 1} \right) \right]$$

$$B_d^P = B_u^n = \tilde{\Sigma}_{\pi N} \left[1 - (1 - y) \left(\frac{z - 1}{z + 1} \right) \right]$$

$$B_s^P = B_s^n = \tilde{\Sigma}_{\pi N} y, \quad \Sigma_{\pi N} = (m_u + m_d) \tilde{\Sigma}_{\pi N}$$

Largest uncertainty from strangeness content of nucleon $y = 1 - \sigma_0 / \Sigma_{\pi N}$

$\Sigma_{\pi N} \sim 59 \text{ MeV}$ can be determined from π -N scattering. $z \simeq 1.49$ and σ_0 can be fit from baryon octet mass differences in chiral pert. theory

Can also calculate σ_0 on the lattice and predict small $\Sigma_{\pi N}$

	$y \rightarrow 0$	$y = 0.06$	$y \rightarrow 1$
$B_u^p = B_d^n$	9.95 (7.59, 12.2)	9.85 (7.51, 12.1)	8.31 (6.34, 10.3)
$B_d^p = B_u^n$	6.67 (5.09, 8.38)	6.77 (5.17, 8.46)	8.31 (6.34, 10.3)
$B_s^p = B_s^n$	0	0.499 (0.380, 0.617)	8.31 (6.34, 10.3)

Table: Can end up with either small $\sigma_0 \lesssim \Sigma_{\pi N}$ or $\sigma_0 \sim \Sigma_{\pi N}$. We assume the central value for $\Sigma_{\pi N}$ of 59 MeV, with the numbers in parentheses indicating the 2σ range for $\Sigma_{\pi N}$ (45 MeV, 73 MeV), see Alarcon, Camalich, Oller 1110.3797.

$$B_{q=c,b,t}^N = \frac{2}{27} \frac{m_N}{m_q} f_g^N, \quad f_g^N = 1 - \sum_{q=u,d,s} f_q^N$$

Quark loops could couple heavy flavor squarks to gluon content in nucleon

Recall, for squark mixing, we have $\mathcal{M}_{Xq \rightarrow Xq} \sim m_q$, so $q = c, b, t$ contributions to σ_{SI}^N will be suppressed by m_q^{-2} without MFV couplings.

Calculate cross section and check dipole moments

$$\sigma_{SI}^N = \frac{\mu_p^2}{4\pi} \left\{ \sum_q g^2 Y_L Y_{Rq} \sin(2\phi_{\tilde{q}}) \left[\frac{1}{(m_{\tilde{q}_1}^2 - m_X^2)} - \frac{1}{(m_{\tilde{q}_2}^2 - m_X^2)} \right] B_q^N \lambda_q \right\}^2$$

where λ_q accounts for running from the weak scale. For $m_X \ll m_{\tilde{q}_1} \ll m_{\tilde{q}_2}$

$$\frac{\Delta a}{m_q} \sim \frac{m_X}{16\pi^2 m_{\tilde{q}_1}^2} g^2 Y_L Y_{Rq} \sin(2\phi_{\tilde{q}})$$

$$\sigma_{SI}^N \sim (1.1 \times 10^9 \text{ pb GeV}^2) \left(\sum_q \frac{\Delta a_q}{m_q} \frac{B_q^N}{0.5} \right)^2 \left(\frac{m_X}{50 \text{ GeV}} \right)^{-2}$$

Direct detection already rules out models with $\Delta a_q (\text{GeV}/m_q) \gtrsim 10^{-9}$

No contribution to quark EDM and quark MDM limits are relatively weak

LEP constrains current quark moments by checking Γ_Z contributions and

LHC constrains chromomagnetic moments; most stringent $\Delta a_q \lesssim 10^{-5}$

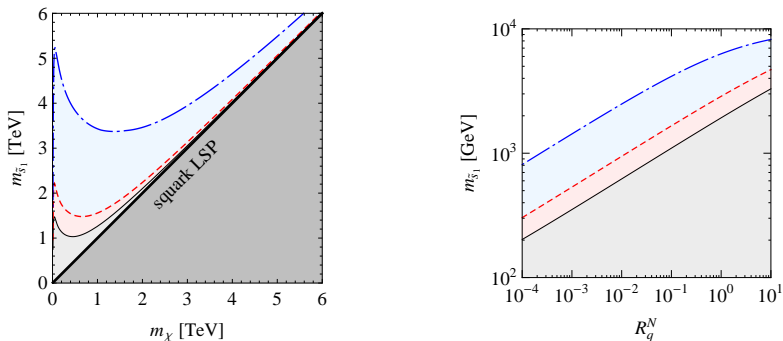
Dependence on model parameters with minimal $B_s^N = 0.5$ 

Figure: Sensitivity of direct detection in the $(m_\chi, m_{\tilde{s}_1})$ plane assuming maximal mixing (left) and in the $(R_q^N, m_{\tilde{s}_1})$ plane with $R_q^N \equiv Y_{Rq}^2 \sin^2(2\phi_{\tilde{q}})(B_q^N)^2 \lambda_q^2$ and $m_\chi = 50$ GeV (right). We assume one light strange squarks and $m_{\tilde{s}_2} = 10$ TeV. The grey region is ruled out by **LUX**, the red region could be ruled out by **300 days of LUX data** and the blue region could be probed by **LZ-7**. Note that, even for $\phi_{\tilde{s}} \sim 0.01$, LZ-7 could probe squark masses not constrained by LHC.

Uncertainty in SI scattering due to strangeness content

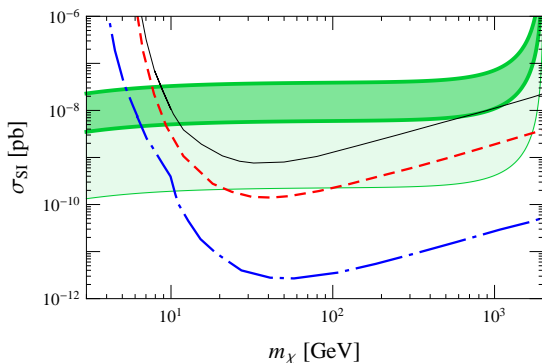


Figure: Sensitivity in the $(m_{\tilde{\chi}}, \sigma_{SI}^N)$ plane with $m_{\tilde{s}_1} = 2$ TeV and maximal mixing. The dark green band indicates the predicted SI-scattering cross section for $\sigma_0 = 27$ MeV and allowing the full 2σ range for $\Sigma_{\pi N}$ of 45 MeV to 73 MeV. The light green band indicates the predicted SI-scattering cross section if one decreases the strangeness content further, to a minimum of $B_s^N = 0.5$.

Outline

- 1 Introduction
- 2 Searches for Light Dark Matter at High Luminosity Colliders
 - Model Independent Constraints on Effective Operators
 - Single Photon Decays of Heavy Quarkonium
 - Results and Analysis
- 3 A Strange Brew in the Incredible Bulk
 - Model Framework
 - Strange Squark Scattering
 - Sensitivity of Direct Detection
- 4 **Cosmological Constraints on Decaying Ensembles**
 - **Single Component DM and Multicomponent DM**
 - **Light Element Abundances**
- 5 Summary and Outlook

Long-lived particles, but not with $\tau \gg t_{now}$

Neutralino LSP with gravity mediated SUSY breaking

- Weak scale gravitino
- Long-lived due to Planck suppressed interactions

Dynamical dark matter

- Ensemble of decaying particles
- Hyperstable fields provide for relic abundance
- Imply existence of more massive, less stable species

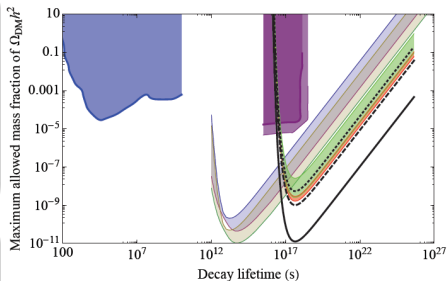


Figure: Fraction of dark matter density allowed by various constraints for decaying species of a particular lifetime and typical masses, see Slatyer 1211.0283.

NLSP \tilde{G} decays after BBN can affect light elements

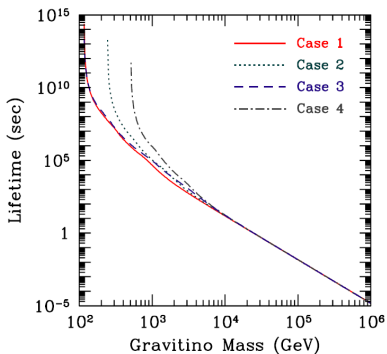


Figure: Gravitino lifetimes for several canonical mSUGRA cases. Consider case 4 with $m_{1/2} = 1.2$ TeV, $m_0 = 0.8$ TeV, $A_0 = 0$, $\tan \beta = 45$, $\mu = -1315$ GeV, see Kawasaki et. al. 0804.3745.

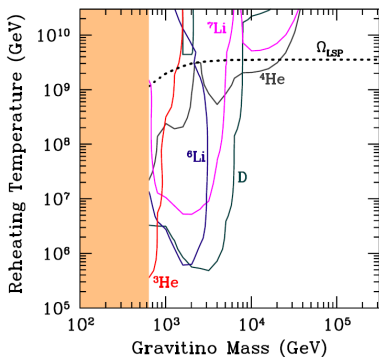
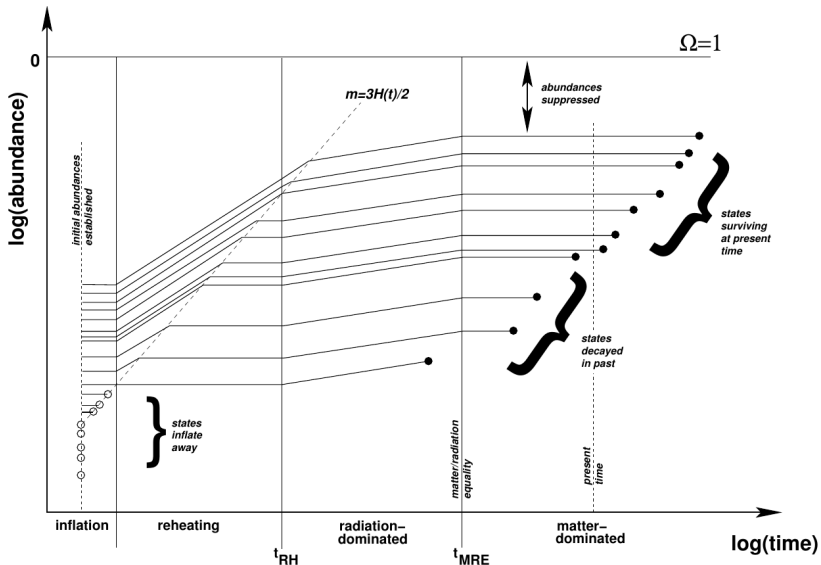


Figure: Upper bound on reheat temperature $\sim \Omega_{3/2}$ constrained by dissociation of light elements due to electromagnetic and hadronic cascades induced by gravitino decays.

Multicomponent ensemble that balances Γ_X and Ω_X 

Electromagnetic processes in the early universe

Fast cascade processes

Pair production, $\gamma\gamma_{BG} \rightarrow e^+e^-$, and inverse Compton scattering, $e^\pm\gamma_{BG} \rightarrow e^\pm\gamma$, rapidly redistribute injected energy above pair production threshold $\sim m_e^2/22T$

Processes that ruin BBN or CMB

Photodisassociation of light elements produced during BBN and photoionization of neutral hydrogen (and helium) after recombination, expanding last scattering surface.

Cooling processes

Photon-photon scattering, $\gamma\gamma_{BG} \rightarrow \gamma\gamma$, for energies above $\sim m_e^2/80T$, and pair production off nuclei, $\gamma N \rightarrow e^+e^-N$, further degrade photon spectrum

Thermalization processes

(Double) Compton scattering, $\gamma e_{BG}^\pm \rightarrow (\gamma)\gamma e^\pm$ and bremsstrahlung, $e^\pm N^\pm \rightarrow e^\pm N^\pm \gamma$, will keep background photons in thermal and kinetic equilibrium.

Consider photonically decaying ensembles after t_{BBN}

$$m_i = m_0 + n^\delta \Delta m$$

$$\Omega_i = \Omega_0 (m_i/m_0)^\alpha$$

$$\Gamma_i = \Gamma_0 (m_i/m_0)^\gamma$$

Parametrizing the ensemble

- Motivated by models with "dark tower" of KK modes
- Only consider $\alpha < 0$, $\gamma > 0$
- Normalize Ω_0 to get relic density from $\tau_i > t_{now}$
- Assume $m_0 = \Delta m \sim 0.1 \text{ keV}$
- Set $\tau_0 \sim t_{now}$, $\delta = 1.5$

Photodisintegration $a(\gamma, b)c$

For comoving densities $Y = n/n_B$,

$$\delta Y_a \sim -N_\gamma Y_i Y_a \frac{\sigma_{a(\gamma,b)c}}{\sigma_{therm}}$$

$N_\gamma \simeq$ average number of photons from EM cascade due to uniform decay of ensemble component

Important processes

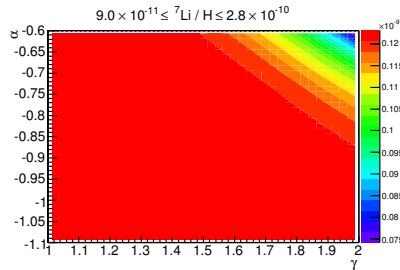
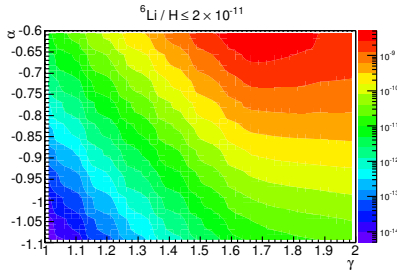
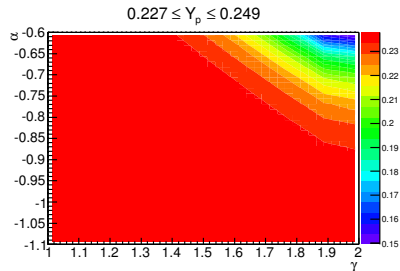
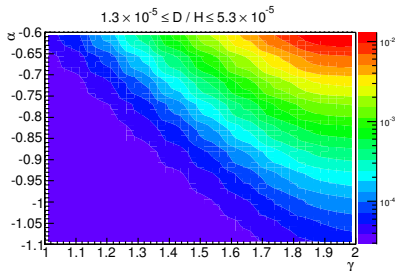
${}^4\text{He}$ most abundant "target"

Overproduction of d : ${}^4\text{He}(\gamma, d)d$

Secondary production of ${}^6\text{Li}$:

${}^4\text{He}(\gamma, n){}^3\text{He} \rightarrow {}^4\text{He}({}^3\text{He}, p){}^6\text{Li}$

$$m_i = m_0 + n^\delta \Delta m, \Omega_i = \Omega_0 (m_i/m_0)^\alpha, \tau_i = \tau_0 (m_i/m_0)^{-\gamma}$$



Given unusual DM paradigms, we reexamined constraints

Light Dark Matter

- Complementary constraints at e^+/e^- colliders
- Set limits on invisible branching fractions and interaction strength for all dimension 6 or lower operators

Strange Dark Matter

- Relaxed MFV in MSSM
- Investigated direct detection
- Can be more sensitive to light squarks than LHC searches
- Light squark coannihilation

Dynamical Dark Matter

- DDM provides for application of decaying DM constraints to multicomponent scenarios
- CMB ionization relevant constraint for viable DM candidate ensembles
- Consider other decay channels and indirect detection constraints
- Calculate with nonuniform decays and redshift dependence

Thank you!



"I can't tell you what's in the dark matter sandwich. No one knows what's in the dark matter sandwich."

Complementary constraints on effective operators

Structure	Invisible	Radiative	s-wave	Scattering
F5 $(1/\Lambda^2)\bar{X}\gamma^\mu X\bar{q}\gamma_\mu q$	$(1^{--}, 1, 0)$	$(0^{++}, 1, 1)$ $(0^{-+}, 0, 0)$ $(1^{++}, 1, 1)$	Yes	SI
F9 $(1/\Lambda^2)\bar{X}\sigma^{\mu\nu} X\bar{q}\sigma_{\mu\nu} q$	$(1^{--}, 1, 0)$ $(1^{+-}, 0, 1)$	$(0^{++}, 1, 1)$ $(0^{-+}, 0, 0)$	Yes	SD

$\Upsilon(1S) \rightarrow \bar{X}X$ related decays

Particular combinations of bound states and final states constrain operators with SM bilinears which can annihilate (J^{PC}, S, L) mesons

$$h_b(1P) \rightarrow \gamma \bar{X}X, \quad \chi_{b0}(1P) \rightarrow \bar{X}X,$$

$$\eta_b(1S) \rightarrow \bar{X}X, \quad \chi_{b1}(1P) \rightarrow \bar{X}X$$

Direct and indirect detection

- s-wave annihilation can yield constraints from dSphs and CMB ionization history
- Velocity independent spin-independent or dependent scattering off of nucleons

Need to approximate limits on $\Upsilon(1S) \rightarrow \gamma \bar{X} X$ decays

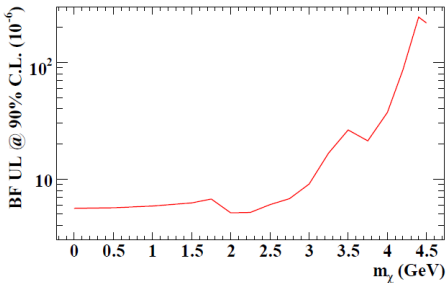
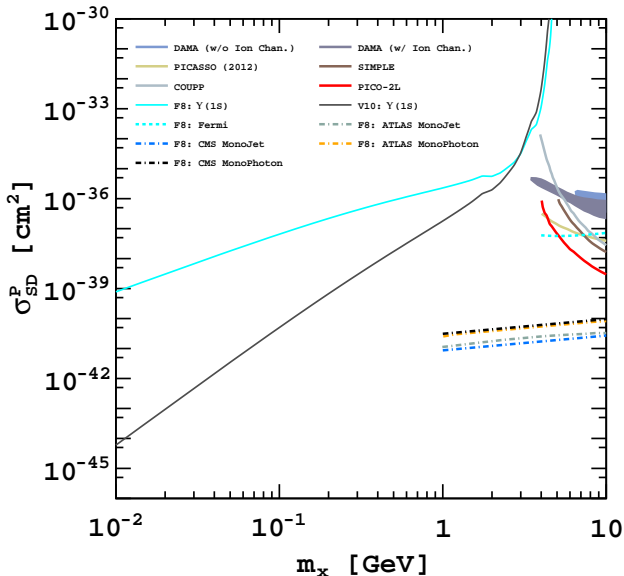


Figure: Limits on $\mathcal{B}(\gamma \bar{X} X)$ for s -wave DM-SM coupling assuming scalar DM, see BaBar 1007.4646. This corresponds to a limit on our S1 and (S2) interaction structures, $\phi^{(\dagger)} \phi \bar{q} (\gamma^5) q$, which turn out to have identical branching fractions.

Interpret S1/S2 limits for operator i

- Calculate partial branching fractions $\mathcal{B}_i^{pol}(\gamma \bar{X} X)$ given polarized initial bound state
- For photon cuts, θ_0 and ω_0 , we define an efficiency for each interaction structure, $\mathcal{F}_i(\theta_0, \omega_0) = \mathcal{B}_i^{pol}(\theta_0, \omega_0) / \mathcal{B}_i$
- Multiply the limits on S1/S2 by $\mathcal{F}_{S1,S2}$, for limits on a partial branching fraction proportional to the number of events
- Product of S1/S2 limits and $\mathcal{F}_{S1,S2} / \mathcal{F}_i$ yields limits on i

$\Upsilon(1S)$ Complementary Bounds on DM-p SD Scattering



Need maximal mixing and $\bar{X}X \rightarrow \tau\tau, \mu\mu$ for relic density

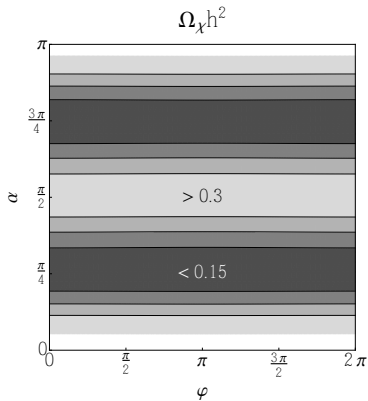


Figure: Bino relic abundance assuming smuon mixing with $m_X = 100$ GeV, $m_{\tilde{\mu}_1} = 120$ GeV and $m_{\tilde{\mu}_2} = 300$ GeV.

$$L_{int} = \lambda_L \tilde{l}_L \bar{\tilde{X}} P_L l + \lambda_R \tilde{l}_R \bar{\tilde{X}} P_R l$$

$$+ \lambda_L^* \tilde{l}_L^* \tilde{X} P_L l + \lambda_R^* \tilde{l}_R^* \tilde{X} P_R l$$

$$\lambda_L = \sqrt{2} g Y_L e^{i\phi/2}$$

$$\lambda_R = \sqrt{2} g Y_R e^{-i\phi/2}$$

$$\begin{bmatrix} \tilde{l}_1 \\ \tilde{l}_2 \end{bmatrix} = \begin{bmatrix} \cos \alpha & -\sin \alpha \\ \sin \alpha & \cos \alpha \end{bmatrix} \begin{bmatrix} \tilde{l}_L \\ \tilde{l}_R \end{bmatrix}$$

L-R mixing angle α and CP-violating phase ϕ , which has been absorbed into λ . Y_L and Y_R are hypercharge and g is the hypercharge coupling.

Dipole moments constrain mixing

Rule out \tilde{e} , constrain $\tilde{\mu}$, allow $\tilde{\tau}$

Dipole moment contributions from L-R slepton mixing

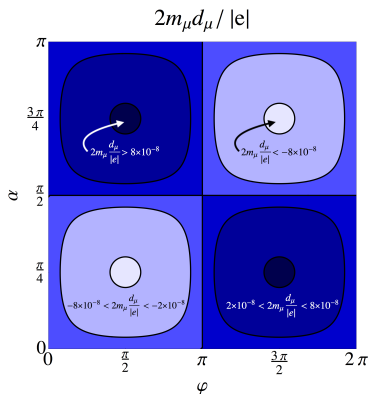


Figure: Muon electric dipole moment contribution assuming smuon mixing with $m_X = 100$ GeV, $m_{\tilde{\mu}_1} = 120$ GeV and $m_{\tilde{\mu}_2} = 300$ GeV. All unconstrained.

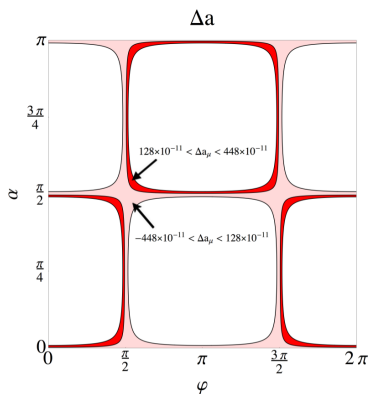


Figure: Muon magnetic dipole moment contribution either fully accounting for measured value (red) or only similar in magnitude (pink).

Dependence on model parameters with minimal $B_s^N = 0.5$

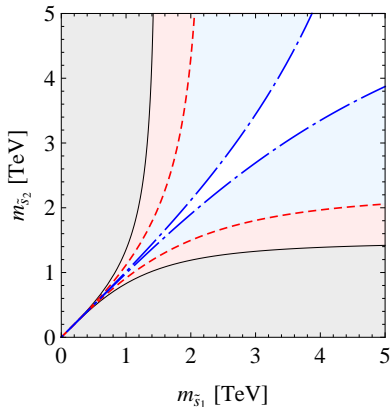


Figure: Sensitivity of direct detection in the $(m_{\tilde{\chi}_1}, m_{\tilde{\chi}_2})$ plane assuming maximal mixing and $m_\chi = 50$ GeV. The grey region is ruled out by **LUX**, the red region could be ruled out by **300 days of LUX data** and the blue region could be probed by **LZ-7**.

Electromagnetic injection heats e_{BG}^- , which then heat γ_{BG}

Compton scattering maintains kinetic equilibrium and generates effective chemical potential, μ -type distortion

$$\frac{d\mu}{dt} = \frac{d\mu_{inj.}}{dt} - \mu(\Gamma_{DC} + \Gamma_{BR})$$

$$\frac{d\mu_{inj.}}{dt} \sim \sum_i \left[\frac{3}{\rho_\gamma} \Gamma_i \rho_i - \frac{8}{n_\gamma} \Gamma_i \frac{\rho_i}{m_i} \right]$$

y_c -type distortion after Compton scattering becomes inefficient

$$\frac{dy_c}{dt} \sim \frac{1}{\rho_\gamma} \sum_i \Gamma_i \rho_i$$

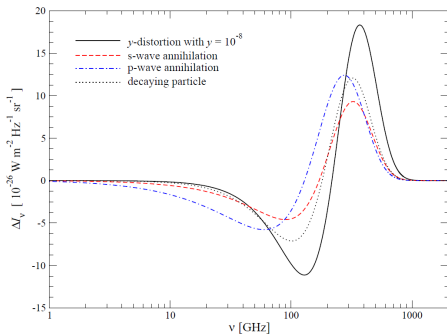
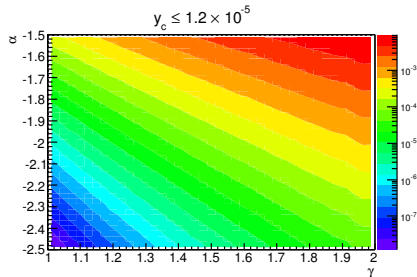
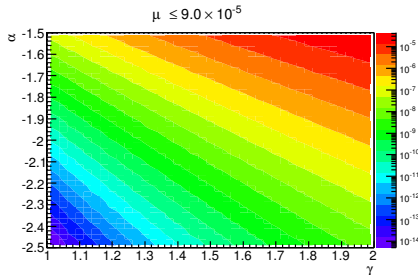


Figure: Distortions to the average photon occupation number plotted as an intensity for different injection histories, all with total injected energy $\Delta\rho_\gamma/\rho_\gamma \sim 10^{-8}$. Decaying particle has $\tau \sim 4 \times 10^8$ s, see Chluba 1304.6120.

$$m_i = m_0 + n^\delta \Delta m, \Omega_i = \Omega_0 (m_i/m_0)^\alpha, \tau_i = \tau_0 (m_i/m_0)^{-\gamma}$$



- Scans over ensembles with $m_0 = \Delta m \sim 0.1 \text{ keV}$, $\tau_0 \sim t_{now}$, $\delta = 1.5$
- y_c more constraining than μ or light elements for "front loaded" ensembles with more abundant lighter, longer-lived components
- Uniform decay approximation ignores possible coherent contributions
- Even taking coherence into account, DDM models underconstrained

CMB ionization constrains viable DM candidate ensembles

Expand last scattering surface

- Electromagnetic cascade and cooling processes degrade photons to ionization energy
- Photons that cool on time scales $\sim t_H$ ionize HI
- Constrains injection rate at recombination from components with $\tau_i \gg t_{now}$

Limits total instantaneous rate

$$\sum_i \Omega_i \Gamma_i \lesssim 2.53 \times 10^{-26} \text{ s}^{-1}$$

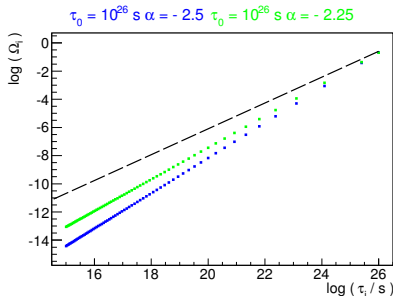
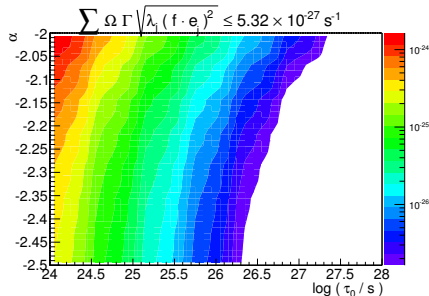
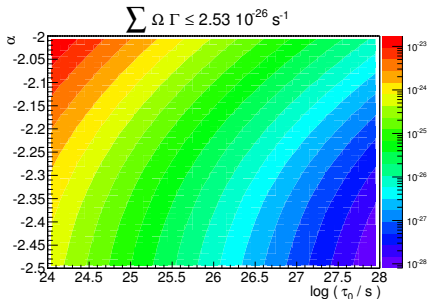


Figure: Two DDM ensemble model points and single component limits from Slatyer 1211.0283. Individual component decays from both ensembles would be permitted by single component limits, but only $\alpha = -2.5$ ensemble is allowed.

$$m_i = m_0 + n^\delta \Delta m, \Omega_i = \Omega_0 (m_i/m_0)^\alpha, \tau_i = \tau_0 (m_i/m_0)^{-\gamma}$$



- Less sensitive to earlier decaying components, fix $\gamma = 2.0$, $\delta = 3.0$
- Left is total injection rate using analytical approximation and right is result of principal component method, Finkbeiner et. al. 1109.6322.
- Decreasing α reduces to single component limits requiring $\tau_0 \gtrsim 10^{26} \text{ s}$
- More dynamical with increasing α , faster injection with decreasing τ_0

Photons from decays $\sim t_{now}$ contribute to diffuse flux

Boltzmann eqn for each component

$$\dot{n}_\gamma + 3Hn_\gamma = 2 \sum_i \Gamma_i \frac{\rho_i}{m_i}$$

$$\frac{dn_\gamma}{dE_\gamma} \sim 6\rho_{c,0} \sum_i \frac{t_{now}}{\tau_i} \frac{\Omega_i}{m_i^2}$$

- Limits instantaneous injection rate today given $\tau_i \gg t_{now}$
- Each component puts flux into a different "bin" with $E_\gamma \sim m_i/2$
- Components do not contribute coherently to the spectrum

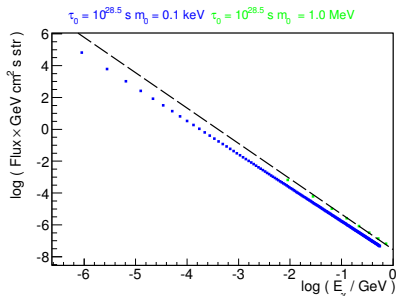
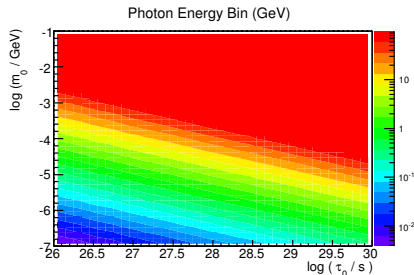
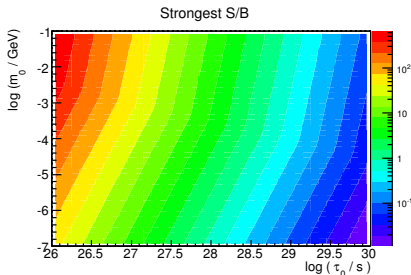


Figure: Diffuse photon flux contributions from dynamical ensembles with $\alpha = -2.1$ and $\gamma = 2$. Dashed line is an approximate combination of power laws for the limits described in Dienes, Thomas 1203.1923 .

$$m_i = m_0 + n^\delta \Delta m, \Omega_i = \Omega_0 (m_i/m_0)^\alpha, \tau_i = \tau_0 (m_i/m_0)^{-\gamma}$$



- Left plot shows the largest ratio of excess flux over observed limits
- Right plot shows the observed E_γ corresponding to largest excess
- $E_\gamma \gg m_0$ suggests departure from single component limits
- Heavier less abundant components subject to more stringent limits

Bound State Decay Matrix Elements

Convolve nonrelativistic bound state wavefunction with $\mathcal{M}(q\bar{q} \rightarrow X\bar{X})$

Since we consider s -wave meson bound states, this convolution depends only on the value of the spatial wavefunction at the origin, $\psi(0)$.

$$\mathcal{M}(\Upsilon(1S) \rightarrow X\bar{X}) = \sqrt{\frac{M_\Upsilon}{2m_b^2}} \int \frac{d^3k}{(2\pi)^3} \tilde{\psi}(k) \mathcal{M}(b\bar{b} \rightarrow X\bar{X})$$

$$\mathcal{B}(\Upsilon(1S) \rightarrow e^+e^-) = 16\pi\alpha^2 Q_b^2 \frac{|\psi_\Upsilon(0)|^2}{\Gamma_\Upsilon M_\Upsilon^2} = 0.0238 \pm 0.0011$$

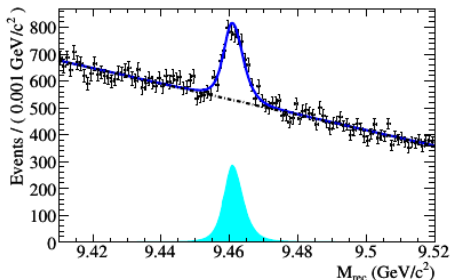
Calculate spatial wavefunctions at the origin with PDG values

- $M_\Upsilon = 9460.30 \pm 0.26$ MeV, $\Gamma_\Upsilon = 54.02 \pm 1.25$ keV
- $M_{J/\psi} = 3096.916 \pm 0.011$ MeV, $\Gamma_{J/\psi} = 92.9 \pm 2.8$ keV

Use $\Upsilon(3S) \rightarrow \pi^+\pi^-\Upsilon(1S)$ to Detect $\Upsilon(1S)$ Peak

$$M_{rec}^2 = s + M_{\pi\pi}^2 - 2\sqrt{s}E_{\pi\pi}^*$$

- M_{rec} recoil mass distribution
- $M_{\pi\pi}$ invariant mass of dipion
- $E_{\pi\pi}^*$ dipion energy $\Upsilon(3S)$ frame
- $\sqrt{s} \sim 10 \text{ GeV}$ $\Upsilon(3S)$ resonance



$$\mathcal{B}(\Upsilon(1S) \rightarrow \text{invisible}) < 3.0 \times 10^{-4}$$

$$\mathcal{B}(J/\psi \rightarrow \text{invisible}) < 7.2 \times 10^{-4}$$

$$\mathcal{B}(\Upsilon(1S) \rightarrow \nu\bar{\nu}) = 9.85 \times 10^{-6}$$

$$\mathcal{B}(J/\psi \rightarrow \nu\bar{\nu}) = 2.70 \times 10^{-8}$$

Figure: Maximum likelihood fit for M_{rec} at BaBar [arXiv:0908.2840]. The total fit (solid line) is composed of nonpeaking background (dashed line) and peaking component (solid filled). Invisible width calculated by subtracting background peak contribution.

Dwarf Spheroidal Galaxies

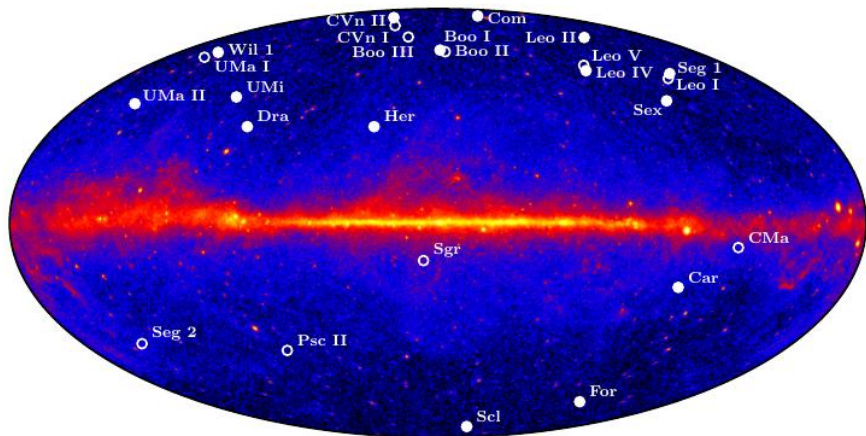


Figure: Known dwarf spheroidal satellite galaxies of the Milky Way overlaid on the 4-year Fermi-LAT photon count map (photons must have energy greater than $E_{thr} \sim 1$ GeV) [arXiv:1310.0828]. In our analysis, we use 2-year Fermi-LAT data [arXiv:1108.3546] for bounds independent of DM density distribution.

Limits on Diffuse Gamma Ray Flux

$$\mu(\Phi_{PP}, J) = (A_{\text{eff}} T_{\text{obs}}) \times \frac{\langle \sigma_{AV} \rangle}{8\pi m_X^2} \int_{E_{\text{thr}}}^{m_X} \frac{dN_\gamma}{dE_\gamma} dE_\gamma \times \int_{\Delta\Omega} \int_l \rho_X^2 dl d\Omega$$

Expected number of signal events factorizes nicely into **particle physics** and **DM astrophysics**, with annihilation cross section $\langle \sigma_{AV} \rangle$ and associated photon spectrum dN_γ/dE_γ along line of sight l over solid angle $\Delta\Omega$.

Dwarf Spheroidal Galaxies

- Large DM content inferred by observation of baryons
- Lack of SM astrophysical production mechanisms
- Correlate with DM annihilation signals at Galactic center

Navarro-Frenk-White DM Density Profile

$$\rho_X(r) = \frac{\rho_X r_s^3}{r(r_s + r)^2}$$

Particle Physics Constraint from Stacked Analysis of Dwarf Spheroidal Galaxies

$$\Phi_{PP} < 5.0_{-4.5}^{+4.3} \times 10^{-30} \text{ cm}^3 \text{ s}^{-1} \text{ GeV}^{-2}$$

Bounds on DM Annihilation

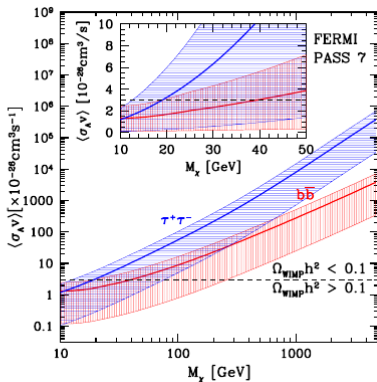
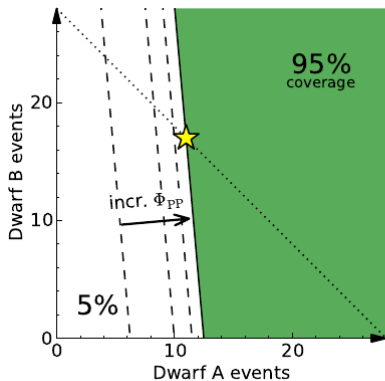


Figure: **Left:** Example of stacked analysis of the gamma ray events from two dwarf spheroidal galaxies weighted by ratio of $A_{\text{eff}} T_{\text{obs}} J$ to expected empirical background. Unweighted analysis is dotted line and data is the star. **Right:** Corresponding limits on DM annihilation cross section. Dashed line shows cross section required for a WIMP to account for the relic abundance [arXiv:1108.2914].

Constraints on $q\bar{q}$ Annihilation Channels

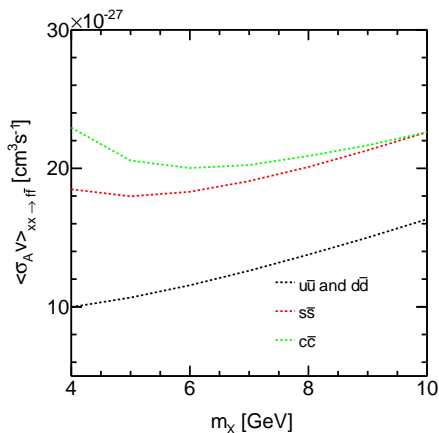


Figure: Bounds on the annihilation cross section, $\langle\sigma_{AV}\rangle$, for DM of mass m_χ annihilating to quarks in dwarf spheroids.

Remarks

- For $m_\chi \gtrsim 5$ GeV, bounds strengthen with smaller m_χ due to larger number density
- For $m_\chi \lesssim 5$ GeV, bounds weaken due to $E_{thr} \sim 1$ GeV and threshold for $c\bar{c}$, $s\bar{s}$
- Need $E_\gamma > E_{thr}$ to contribute
- For $m_\chi \lesssim 4$ GeV, quark energy near hadronization scale
- $u\bar{u}$ and $d\bar{d}$ annihilation channels are visually identical
- CMB constrains s-wave annihilation at recombination

DM Scattering Off of Heavy Nuclei

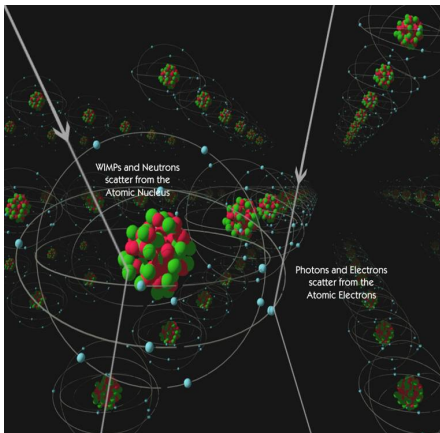


Figure: Weak and electromagnetic recoils off of heavy nuclei by DM and radiative background, respectively.

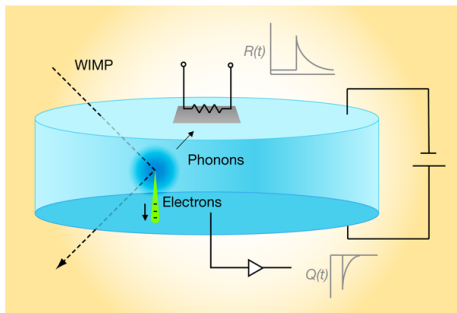


Figure: Schematic of individual detector within CDMS. Ionization products of nuclear recoils drift to one face of the detector due to a weak electric field. Phonons reach the other face and heat a superconducting aluminum layer, causing a change in resistance [K. van Bibber].

Bounds on DM-nucleon Scattering

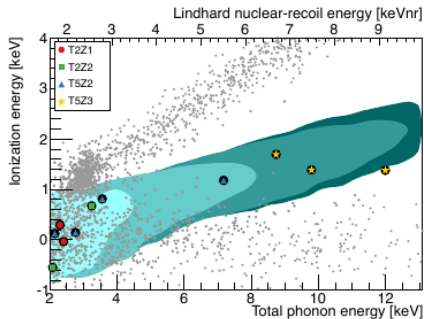


Figure: SuperCDMS low mass WIMP search [arXiv:1402.7137]. Gray dots are all single-scatter events to pass data-quality selection criteria. Large circles are WIMP candidates. Contours are 95 % CL for $m_\chi = 5, 7, 10, 15$ GeV.

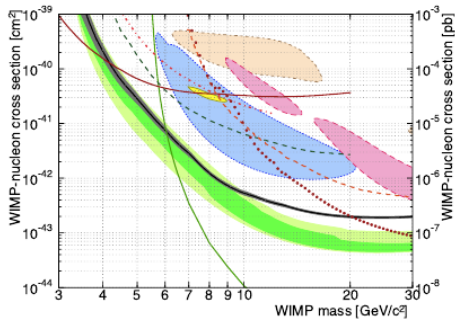


Figure: 90 % CL limits set by SuperCDMS (black) and LUX (green). Green bands are pre-blinding expected sensitivity of SuperCDMS. Disagreement between limit and sensitivity is due to T5Z3 events, which were disregarded.

Relevant Effective Contact Operators

Name	Interaction Structure	Annihilation	Scattering
F5	$(1/\Lambda^2)\bar{X}\gamma^\mu X\bar{q}\gamma_\mu q$	Yes	SI
F6	$(1/\Lambda^2)\bar{X}\gamma^\mu\gamma^5 X\bar{q}\gamma_\mu q$	No	No
F9	$(1/\Lambda^2)\bar{X}\sigma^{\mu\nu} X\bar{q}\sigma_{\mu\nu} q$	Yes	SD
F10	$(1/\Lambda^2)\bar{X}\sigma^{\mu\nu}\gamma^5 X\bar{q}\sigma_{\mu\nu} q$	Yes	No
S3	$(1/\Lambda^2)\nu\text{Im}(\phi^\dagger\partial_\mu\phi)\bar{q}\gamma^\mu q$	No	SI
V3	$(1/\Lambda^2)\nu\text{Im}(B_\nu^\dagger\partial_\mu B^\nu)\bar{q}\gamma^\mu q$	No	SI
V5	$(1/\Lambda)(B_\mu^\dagger B_\nu - B_\nu^\dagger B_\mu)\bar{q}\sigma^{\mu\nu} q$	No	SD
V7	$(1/\Lambda^2)B_\nu^{(\dagger)}\partial^\nu B_\mu\bar{q}\gamma^\mu q$	No	No
V9	$(1/\Lambda^2)\epsilon^{\mu\nu\rho\sigma}B_\nu^{(\dagger)}\partial_\rho B_\sigma\bar{q}\gamma_\mu q$	No	No

Table: EFT operators which can mediate the decay of a $J^{PC} = 1^{--}$ quarkonium bound state. We also indicate if the operator can permit an s -wave dark matter initial state to **annihilate** to $q\bar{q}$; if so, then a bound can also be set by indirect observations of photons originating from dwarf spheroidals. Lastly, we indicate if the operator can mediate velocity-independent **scattering** [arXiv:1305.1611].

Relevant Bilinears for Our Matrix Elements

Bilinear	C	P	J	State
$\bar{\psi}\gamma^i\psi$	-	-	1	$S = 1, L = 0, 2$
$\bar{\psi}\gamma^i\gamma^5\psi$	+	+	1	$S = 1, L = 1$
$\bar{\psi}\sigma^{0i}\psi$	-	-	1	$S = 1, L = 0, 2$
$i\text{Im}(\phi^\dagger\partial^i\phi)$	-	-	1	$S = 0, L = 1$
$i\text{Im}(B_\nu^\dagger\partial^i B^\nu)$	-	-	1	$S = 0, L = 1; S = 2, L = 1, 3$
$i(B_i^\dagger B_0 - B_0^\dagger B_i)$	-	-	1	$S = 0, L = 1; S = 2, L = 1, 3$
$-\epsilon^{0ijk} B_0\partial_j B_k$	+	+	1	$S = 2, L = 2$
$B_\nu\partial^\nu B_i$	+	-	1	$S = 1, L = 1$

Table: In general, allow for violation of C and/or P , but must conserve total J . Fermionic bilinears with $J^{PC} = 1^{--}$ are for bound state quarkonium or dark matter. F5 and F9 should have two terms in their respective matrix elements for $L = 0$ and $L = 2$. Interaction structures with scalar or vector DM have matrix elements that are necessarily **velocity suppressed**. Bounds on V5 will be enhanced since it is **dimension 5**. Conjugate decay matrix elements for DM annihilation.

Branching Fractions to Scalar and Fermionic Dark Matter

$$\mathcal{B}_{F5}(\bar{X}X) = \frac{\mathcal{B}(e^+e^-)M^4}{16\pi^2\alpha^2Q^2\Lambda^4} \left(1 - \frac{4m_X^2}{M^2}\right)^{1/2} \left(1 + \frac{2m_X^2}{M^2}\right)$$

$$\mathcal{B}_{F6}(\bar{X}X) = \frac{\mathcal{B}(e^+e^-)M^4}{16\pi^2\alpha^2Q^2\Lambda^4} \left(1 - \frac{4m_X^2}{M^2}\right)^{3/2}$$

$$\mathcal{B}_{F9}(\bar{X}X) = \frac{\mathcal{B}(e^+e^-)M^4}{8\pi^2\alpha^2Q^2\Lambda^4} \left(1 - \frac{4m_X^2}{M^2}\right)^{1/2} \left(1 + \frac{8m_X^2}{M^2}\right)$$

$$\mathcal{B}_{F10}(\bar{X}X) = \frac{\mathcal{B}(e^+e^-)M^4}{8\pi^2\alpha^2Q^2\Lambda^4} \left(1 - \frac{4m_X^2}{M^2}\right)^{3/2}$$

$$\mathcal{B}_{S3}(\bar{X}X) = \frac{\mathcal{B}(e^+e^-)M^4}{256\pi^2\alpha^2Q^2\Lambda^4} \left(1 - \frac{4m_X^2}{M^2}\right)^{3/2}$$

We have written the decay rates in terms of $\mathcal{B}(e^+e^-)$ instead of $\psi(0)$. Note $q = b$ for $\Upsilon(1S)$ or $q = c$ for J/ψ . F6, F10 and S3 are **p-wave** suppressed because the DM bilinears can't annihilate an $L = 0$ state.

Branching Fractions to Vector Dark Matter

$$\mathcal{B}_{V3}(\bar{X}X) = \frac{\mathcal{B}(e^+e^-)M^4}{128\pi^2\alpha^2Q^2\Lambda^4} \left(1 - \frac{4m_X^2}{M^2}\right)^{3/2} \left(1 + \frac{M^4}{8m_X^4} \left(1 - \frac{2m_X^2}{M^2}\right)^2\right)$$

$$\mathcal{B}_{V5}(\bar{X}X) = \frac{\mathcal{B}(e^+e^-)M^2}{16\pi^2\alpha^2Q^2\Lambda^2} \left(1 - \frac{4m_X^2}{M^2}\right)^{3/2} \frac{M^2}{m_X^2} \left(1 + \frac{M^2}{4m_X^2}\right)$$

$$\mathcal{B}_{V7}(\bar{X}X) = \frac{\mathcal{B}(e^+e^-)M^4}{64\pi^2\alpha^2Q^2\Lambda^4} \left(1 - \frac{4m_X^2}{M^2}\right)^{3/2} \frac{M^2}{m_X^2}$$

$$\mathcal{B}_{V9}(\bar{X}X) = \frac{\mathcal{B}(e^+e^-)M^4}{256\pi^2\alpha^2Q^2\Lambda^4} \left(1 - \frac{4m_X^2}{M^2}\right)^{5/2} \frac{M^2}{m_X^2}$$

Terms in which scale as m_X^{-2} (m_X^{-4}) have one (two) longitudinally polarized vector boson in a final state with total spin $S = 1$ ($S = 0, 2$). Note the constraints from unitarity are trivial in the non-relativistic limit, because the elastic scattering cross section is at threshold [eg arXiv:1403.6610].

Annihilation Cross Sections

$$\begin{aligned}\langle \sigma_A^{F10} v \rangle &= \frac{6}{\pi \Lambda^4} \left(1 - \frac{m_q^2}{m_X^2} \right)^{3/2} m_X^2 \\ \langle \sigma_A^{F9} v \rangle &= \frac{6}{\pi \Lambda^4} \left(1 - \frac{m_q^2}{m_X^2} \right)^{1/2} (m_X^2 + 2m_q^2) \\ \langle \sigma_A^{F5} v \rangle &= \frac{3}{2\pi \Lambda^4} \left(1 - \frac{m_q^2}{m_X^2} \right)^{1/2} (2m_X^2 + m_q^2)\end{aligned}$$

Recall

$$\Phi_{PP} = \frac{\langle \sigma_A v \rangle}{8\pi m_X^2} \int_{E_{thr}}^{m_X} \frac{dN_\gamma}{dE_\gamma} dE_\gamma$$

$$\Phi_{PP} \lesssim 5 \text{ cm}^3 \text{ s}^{-1} \text{ GeV}^{-2}$$

These are the only operators with s -wave meson states and DM initial states. As the meson decay and DM annihilation matrix elements are conjugate, F10 is still **p-wave** suppressed. Note that for the operators we are considering, only fermionic dark matter can annihilate from an s -wave initial state. Assuming universal quark coupling, $u\bar{u}$ and $d\bar{d}$ channel yield the strongest bounds from DM annihilation due to the analysis threshold.

$\Upsilon(1S)$ Mediator Scale

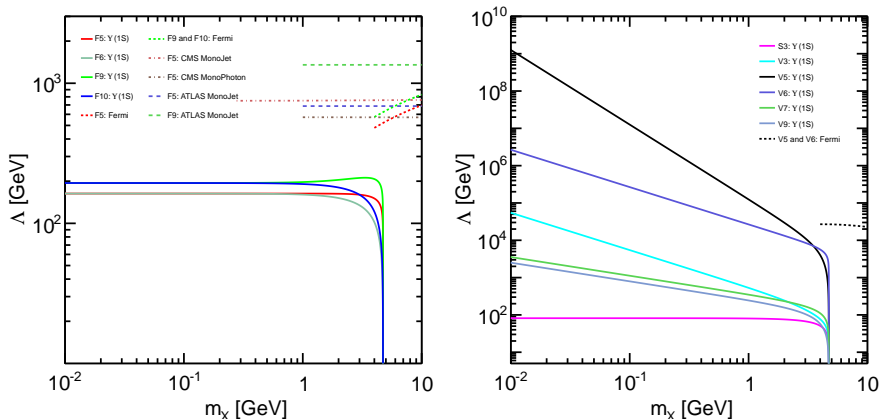


Figure: Bounds on the mediator scale, Λ , for fermionic and scalar DM (left panel) and vector DM (right panel) of mass m_χ arising from constraints on $\Upsilon(1S) \rightarrow \text{nothing}$ decays, from constraints on DM annihilation to light quarks in dwarf spheroidal galaxies, and from monojet/photon searches at LHC.

Scattering Cross Sections

We are looking for velocity independent scattering off of protons

$$\sigma_{SI}^p \sim \mu_p^2 \left| \sum_q \frac{B_q^p}{m_X m_q} \mathcal{M}_{Xq \rightarrow Xq} \right|^2, \quad \sigma_{SD}^p \sim \mu_p^2 \left| \sum_q \frac{\delta_q^p}{m_X m_q} \mathcal{M}_{Xq \rightarrow Xq} \right|^2$$

$$\sigma_{SI}^{F5} = \frac{\mu_p^2}{\pi \Lambda^4} (B_u^p + B_d^p)^2$$

$$\sigma_{SI}^{S3} = \sigma_{SI}^{V3} = \frac{\mu_p^2}{4\pi \Lambda^4} (B_u^p + B_d^p)^2$$

$$\sigma_{SD}^{F9} = \frac{12\mu_p^2}{\pi \Lambda^4} (\delta_u^p + \delta_d^p)^2$$

$$\sigma_{SD}^{V5} = \frac{2\mu_p^2}{\pi \Lambda^2 m_X^2} (\delta_u^p + \delta_d^p)^2$$

Form Factors and Comments

- $B_u^p = B_d^n = 2$, $B_u^n = B_d^p = 1$
- $\delta_u^p = 0.54_{-0.22}^{+0.09}$, $\delta_d^p = -0.23_{-0.16}^{+0.09}$
- Need universal coupling to u , d
- Enhancement from longitudinal polarization of **vector** LDM
- Enhancement from **dimension 5**

$\Upsilon(1S)$ Complementary Bounds on Dark Matter Scattering

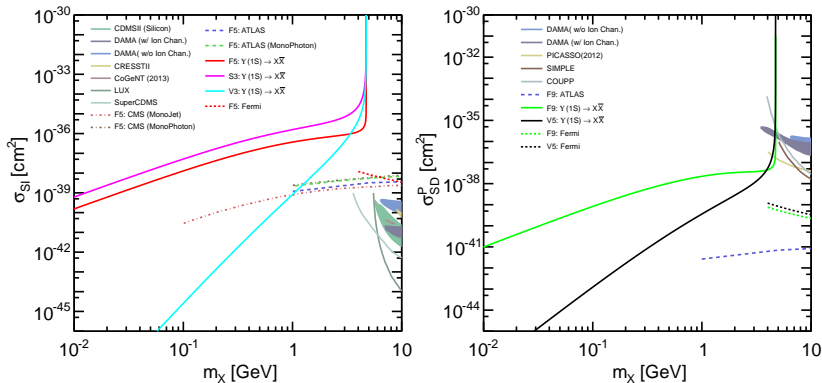


Figure: DM-p SI (left panel) and SD (right panel) scattering for DM coupling universally to quarks through the indicated effective contact operator. The labeled exclusion contours indicate 90 % CL from limits on invisible decays of $\Upsilon(1S)$, 95 % CL from Fermi constraints, and 90 % CL from monojet searches. Signal regions are also shown, as are the 90 % CL exclusion contours from direct detection.

J/ψ Mediator Scale

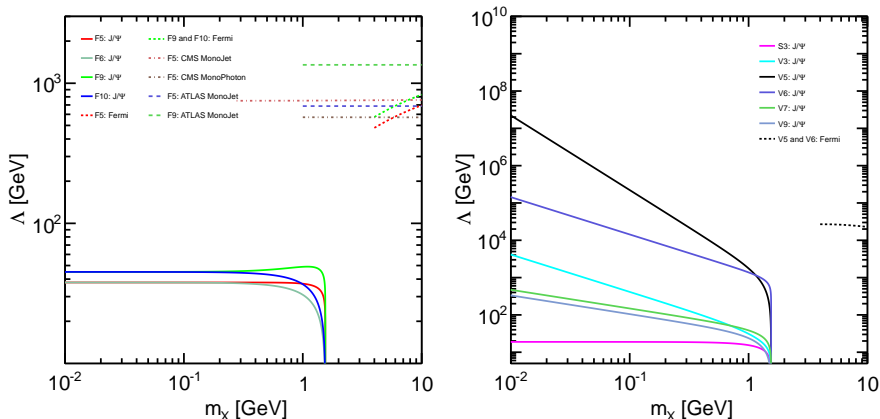


Figure: Bounds on the mediator scale, Λ , for fermionic and scalar DM (left panel) and vector DM (right panel) of mass m_χ arising from constraints on $J/\psi \rightarrow \text{nothing}$ decays, from constraints on DM annihilation to light quarks in dwarf spheroidal galaxies, and from monojet/photon searches at LHC.

J/ψ Complementary Bounds on Dark Matter Scattering

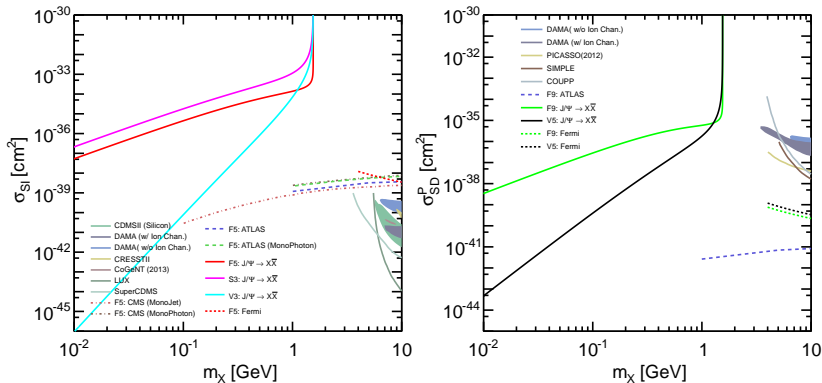


Figure: DM-p SI (left panel) and SD (right panel) scattering for DM coupling universally to quarks through the indicated effective contact operator. The labeled exclusion contours indicate 90 % CL from limits on invisible decays of J/ψ , 95 % CL from Fermi constraints, and 90 % CL from monojet searches. Signal regions are also shown, as are the 90 % CL exclusion contours from direct detection.